

Grid impacts of highway electric vehicle charging and role for mitigation via energy storage

Andrew M. Mowry^{*}, Dharik S. Mallapragada

MIT Energy Initiative, 77 Massachusetts Avenue, E19-307, Cambridge, MA, 02139, USA

ARTICLE INFO

Keywords:

Electric vehicle charging
Production cost modeling
Congestion management
Energy storage
Demand flexibility

ABSTRACT

Highway fast-charging (HFC) stations for electric vehicles (EVs) are necessary to address range anxiety concerns and thus to support economy-wide decarbonization goals. The characteristics of HFC electricity demand – its relative inflexibility, high power requirements, and spatial concentration – have the potential to adversely impact grid operations as HFC infrastructure expands. Here, we investigate the impacts of scaled-up HFC infrastructure using an operations model of the 2033 Texas power grid with uniquely high spatial and temporal resolution. In the reference EV penetration case corresponding to 3 million passenger EVs on the road, we find that grid-HFC interactions increase system annual operational costs by 8%, or nearly \$2 per MWh of load served. Greater impacts are observed for higher EV penetration cases. The high spatial resolution of the analysis reveals that the majority of increased costs can be attributed to transmission congestion on feeder lines serving a minority of HFC stations. Four-hour battery energy storage is shown to be more effective than demand flexibility as mitigation, due to the long duration of peak charging demand anticipated at HFC stations. Transmission network upgrades can also effectively mitigate grid-HFC interactions. Choosing the most effective mitigation strategy for each station requires a tailored approach.

1. Introduction

The electrification of transportation is key to economy-wide decarbonization. Under 2016 grid conditions, an electric vehicle (EV) would be expected to contribute significantly less lifetime greenhouse gases than an internal combustion vehicle in about 75% of counties in the USA (Wu et al., 2019), and estimates by the IEA (2019), BNEF (2019), and OPEC (2019) indicate that sales of these cleaner vehicles will comprise at least 15%–30% of global passenger vehicle sales by 2030. There are challenges to achieving these estimates. In addition to driving down costs, suppliers must invest in more charging infrastructure to alleviate the “range anxiety” of potential EV owners (MIT, 2019). This infrastructure will lead to significantly increased electricity demand: a recent US-wide study, for example, projects that the electrification of U.S. transportation could increase 2050 demand by 800–1700 TWh/year, or 21–44% of the entire US electricity demand in 2016 (Mai et al., 2018). Meeting this new electricity demand in aggregate can be posed as a question of traditional generation capacity expansion, but a complementary challenge lies in accommodating the spatio-temporal patterns

of electricity demand from EV charging. While the operational impacts on distribution networks from EV charging are well-studied (Arias-Londoño et al. (2020) and Deb et al. (2017) offer reviews), comparatively little attention has been paid to impacts on the transmission-scale grid, and almost none to the impacts caused by charging stations¹ located along inter-city highways. These chargers, termed *highway fast-chargers* (HFCs) in this study, comprised roughly 20% of newly opened public chargers in the U.S. in 2019 (Brown et al., 2020). They represent extremely high-power and largely inflexible charging demands, since drivers mid-journey prioritize low wait times and fast charging, and thus they are potentially disruptive to power grid operations (Burnham et al., 2017). Absent contemplation of these topics, the power grid may not evolve to accommodate sufficient EV charging infrastructure, thereby slowing the adoption of EVs and failing to serve society’s decarbonization goals. This paper investigates the grid operational impacts of HFCs in the context of the bulk electricity system in Texas and potential mitigation strategies to address these impacts.

The problem of managing EV charging load to minimize impacts on the power grid has been studied at the system-level. By assuming a

^{*} Corresponding author.

E-mail address: mowry@mit.edu (A.M. Mowry).

¹ Various terminology is used to characterize EV charging infrastructure. We use “chargers” to refer to the individual connections between EVs and supply equipment, analogous to the pumps at gasoline refueling stations. We use “stations” to refer to collections of these chargers.

degree of flexibility in EV charging demand, Xu et al. (2018) and others have shown that coordinated charging strategies can reduce the aggregate coincident power demand from charging, thereby reducing strain on the grid. Without this flexibility, EV charging demand becomes more problematic: Muratori, 2018 shows how uncoordinated residential charging can overwhelm distribution infrastructure at the neighborhood level. HFC demand could pose a similar problem at a larger scale due to its relative inflexibility, high-power requirements, and spatial concentration, all of which make it more challenging to integrate with the grid (Burnham et al., 2017). These potential impacts can be expected to scale as well, since as EV penetration increases so too will the size of the supporting HFC stations. Taking the Tesla Supercharging network as an example, the peak capacity of each Supercharging station has been growing over time, with Tesla's largest Supercharger station at present with a peak capacity of 14 MW² (Github, 2020). Even at more modest levels of current deployment, the operational challenges that HFC stations may pose have already surfaced. During the Thanksgiving holiday in late November 2019, for example, the Tesla Supercharger stations midway between San Francisco and Los Angeles experienced congestion that was belatedly alleviated by dispatching battery storage mounted on trucks to these locations (Conroy, 2020).

Despite their potential magnitude, the operational impacts of HFCs on the power grid have not been fully studied in the literature. This is in part because such an assessment requires spatially and temporally resolved representations of both the charging demand and of the power grid network, generation, and load, as well as an appropriately realistic power system simulator. This level of detail has so far been demonstrated for small-scale systems consisting of one-to-several charging stations, for which Ma (2019) offers a review, but not for full-scale grids. Four recent studies have come close to the approach needed for this problem, but they simplify the transmission networks using either a copper-plate or zonal approximation, approaches that are not adequate to simulate the true spatial characteristics of HFC stations. Wolinetz et al. (2018) develop a bottom-up EV charging model coupled to a power system operations model that includes hourly generation dispatch, but they use a copper-plate approximation for the transmission network and derive system prices from levelized costs of electricity (LCOE) for grid generation. Heuberger et al. (2020) model the UK grid topology as a system of 29 aggregate nodes and use a commitment and dispatch simulator (ESONE) over representative periods to approximate annual grid operations. Moreover, there is not explicit modeling of fast charging demand. Szinai et al. (2020) use a coupled vehicle traffic simulation model (BEAM) and a grid simulator (PLEXOS) with a zonal representation (25 zones are modeled) of the U.S. Western Interconnect. While they do specifically model fast-charging infrastructure, it is represented coarsely at the zonal level due to the model structure. Similarly, Jenn et al. (2020) analyzed the effects of fast-charging infrastructure in the 2030 US power system using a temporally detailed grid simulator (GOOD), but the model's spatial resolution was kept at the regional level. Furthermore, they focused on the environmental effects of fast-charging, and not the operational costs sustained by the grid.

This paper establishes the importance of detailed spatial resolution to extend the above line of research. We explicitly analyze the operational impacts of locationally resolved HFC stations in the context of the grid operated by the Electric Reliability Council of Texas (ERCOT), which serves the majority of electrical load in Texas. We apply a highly detailed production cost model (PCM) with over 3500 buses and over 9000 transmission lines spanning the ERCOT grid. We use the PCM to evaluate grid dispatch at an hourly resolution for a full year under various scenarios of HFC demand and grid conditions in 2033. The detailed modeling resolution quantifies costs associated with EV adoption that less detailed charger-grid interaction studies fail to capture. Additionally, we investigate mitigation strategies to minimize the cost

impacts of HFC operation, including demand flexibility, co-located battery storage, and transmission reinforcement. Notably, we find that demand flexibility – even if it were practicable for HFCs at modest levels (+/- 1-h flexibility) – is largely ineffective due to the long periods of grid congestion resulting from HFC-grid interactions. Battery storage with 4-h duration represent a more practical and cost-effective strategy for mitigating the grid operational impacts for HFC.

The rest of the paper is outlined as follows. The next section describes the overall methodology including an overview of the PCM used, data to characterize grid operations, and the definition of the EV demand scenarios. This is followed by a discussion of the main grid operation outcomes resulting from serving HFC demand and the impacts of alternative mitigation strategies. We conclude by discussing the policy implications of the findings and areas of future work.

2. Methods

2.1. Overview and data statement

Fig. 1 summarizes the overall approach of the study. We evaluate the grid operational impacts of HFC deployments through a case study of the ERCOT power grid in 2033, for which projections on generation, baseline electricity demand, transmission reinforcements, and EV penetration in the transport sector are available from ERCOT's 2018 Long-Term System Assessment Report (LTSA) (ERCOT, 2018). We assess the overall grid impacts of HFC station operation accompanying rising EV penetration by comparing the outputs of the PCM for 2033 with and without ("Concentrated Case" and "Base Case", respectively, in Fig. 1) HFC demand. To isolate the locational effects of fast-charging on the power system, we evaluate another case ("Distributed Case" in Fig. 1) that distributes HFC demand within each ERCOT weather zone across all the load buses within that zone, in proportion to their original load.³ Through comparison of these three Cases, we decompose the total grid impacts of HFCs into "Zonal Effects" (difference between the Distributed Case and the Base Case) and "Local Effects" (difference between the Concentrated Case and the Base Case). The latter are intended to capture mainly the grid impacts resulting from the spatial concentration of power demand, while the former to capture mainly the grid impacts from an increase in aggregate electricity demand. This decomposition is a main contribution of this study, enabled by the spatial resolution of our model, and it isolates the grid effects of the spatial concentration of HFC power demand.

Our choice of the ERCOT system to study EV charging impacts is informed by several factors: (1) it already contains developed EV charging infrastructure, with new EV registrations 4th highest in the country and comprising 4% of the U.S. total in 2018 (Autoalliance, 2020; DOE, 2020); (2) it is sufficiently large to observe large-scale effects and a variety of local situations, with over 30 million residents (US Census, 2020) and a peak summer demand of about 75 GW (ERCOT, 2020); (3) its power system is electrically and politically isolated from neighboring regions, making its analysis simple without the need to consider import/exports from other states; and (4) the necessary data to conduct this study are available publicly. Finally, our choice of the year 2033 for the simulations is a direct consequence of our choice of the ERCOT system: the 2018 ERCOT LTSA chooses 2033 for its generation, EV, and transmission forecasts, and so do we.

The data, a data dictionary, and analysis scripts used in this study are freely available on Github at https://github.com/mowryand/HFC_grid_impacts, and hosted data referred to in this paper will be cited as (Github, 2020). Academic licenses to the PCM software we used are available at <http://www.psopt.com/contact/>.

³ Refer to the data dictionary on Github (2020) for a description of the weather zones.

² The Firebaugh, CA station.

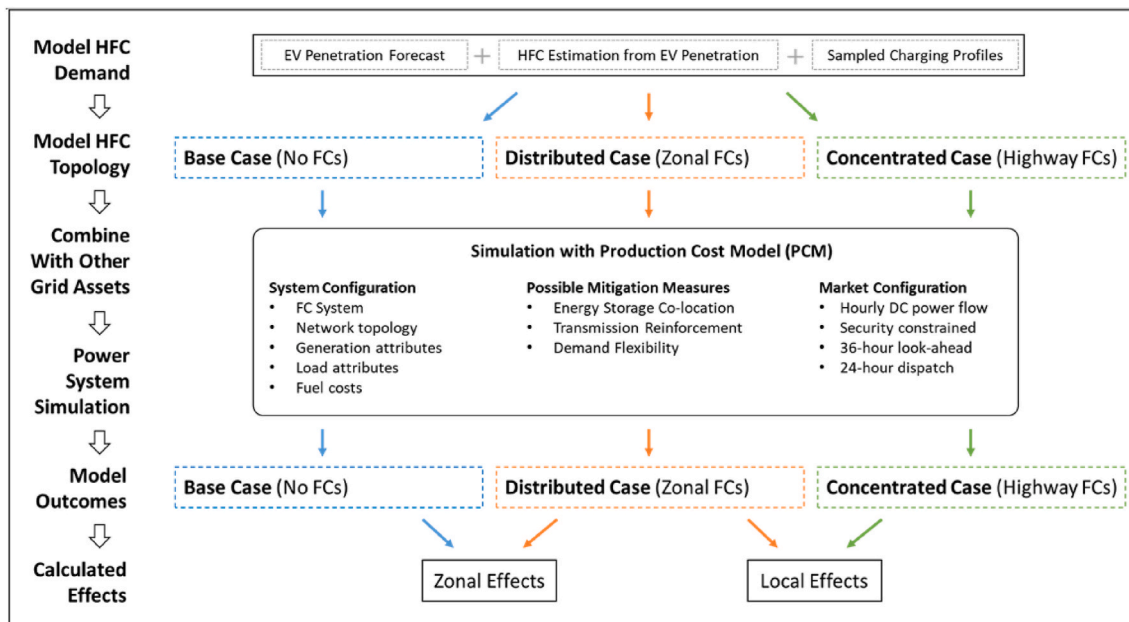


Fig. 1. Schematic representation of scenario modeling approach. The impacts of HFCs can be decomposed into Zonal Effects and Local Effects. These effects are separated by analyzing an intermediate “Distributed Case”, which spreads fast-charging demand to all electrical nodes in a zone, as well as the “Base Case” and “Concentrated Case”, which realistically locates charging demand into few locations along highway corridors. Note: FC = “Fast Charger”.

2.2. Power network data

The modeled ERCOT network includes all transmission, generation, and load operated by ERCOT that interconnects at or above 69 kV (the “wholesale” or “transmission” level). The topological data that identifies the interconnections between generation buses, load buses, and power lines, as well as the physical parameters such as impedance that are necessary to create an electrical model are derived from the network model that ERCOT released for its June 2018 monthly Congestion Revenue Rights (CRR) auction (Github, 2020). This topology contains over 3500 load buses with a median power rating of 7.5 MW, over 9000 transmission lines that range from 69 kV to 345 kV, and close to 750 unique generation units (See Fig. 2, left side.). We construct hourly load schedules at each of the load buses by distributing historical weather zone-level hourly load data from 2017 (Github, 2020) pro-rata according to each load bus’ power rating in the CRR network representation. We assemble generation dispatch characteristics, namely variable operation costs, ramp rates, and min/max power outputs, from the S&P Global SNL power plant database (Github, 2020). Daily natural gas prices at Henry Hub from 2017 were obtained from the US Energy Information Administration (Github, 2020). Uranium, coal, and biomass prices are set at constant levels that reflect average levels in 2017 and that appropriately locate the respective generation in the total ERCOT supply stack (Github, 2020). Wind and solar availability are based on zonal, hourly resource availability for 2013, the latest year of data available from the National Solar Radiation Database (Github, 2020).

We extrapolate the above historically-derived grid modeling parameters to 2033 based on the “Current Trends” scenario of the LTSA (ERCOT, 2018). For generation, the changes include 3 GW of coal retirements, 3 GW of natural gas (combined cycle) additions, and 18 GW of wind and solar additions, most of these in the western areas of the state. To effect these changes, we modify the maximum output of existing generation of the same technology and in the same weather zone. For example, to add 9.2 GW of solar additions in the “Far West” weather zone we increase nameplate capacity of existing solar facilities in the Far West by 9.2 GW. Natural gas prices preserve their historical intra-annual variability but are mean-corrected to the LTSA 2033 assumption of \$4.50/MMBtu. Other fuel prices follow the EIA’s long-term projections,

corresponding to \$1.96/MMBtu for coal and \$0.70/MMBtu for uranium (EIA, 2020a).

For load, we extrapolate monthly system load and peak-demand forecasts from ERCOT’s Long-Term Load Forecast (Github, 2020), available through 2028, using twelve monthly regression models. We then scaled the historical 2017 hourly load data to fit the predicted 2033 load and peak power demand by month and zone. This approach is validated by comparison of our predictions to the LTSA aggregate numbers: our model predicts an annual peak power demand of 96.6 GW and a total annual energy demand of 544 TWh in 2033, compared to the LTSA’s predicted 94.5 GW and 530 TWh. These numbers are exclusive of HFC loading. The combination of load and generation changes in the LTSA base scenario predicts a reserve margin of less than 5%, which is unrealistically low, and thus we increase natural gas peaking capacity to attain a 10% reserve margin, which is consistent with recent trends for ERCOT (Brattle, 2019a).

For transmission, the LTSA identifies several transmission corridors that will need reinforcement over the next decade, most of which serve to export power from the increasingly generation-rich west of the state to the load centers in the east of the state. Without specific identification of these upgrade projects to apply to our model, we used a diagnostic simulation of our modeled Base Case (without HFCs) to identify transmission lines with violated thermal operation limits, and we then upgraded the affected lines as necessary to prevent these violations. As a result, there are no violations in the Base Case. Although this approach may result in an overly reinforced “gold-plated” network, that would only understate the magnitude of our results regarding grid operational impacts of EV penetration.

2.3. EV charging network data

The modeled EV charging network is composed both of a distributed residential charging network and an HFC network. The distributed network is not a special focus of this study and is modeled in relatively low detail: aggregate residential charging load as reported by ERCOT (ERCOT, 2018) is distributed among all load buses on the power network in the same pro-rata fashion as other system load, and this aggregate load is shaped to hourly demand according to the median

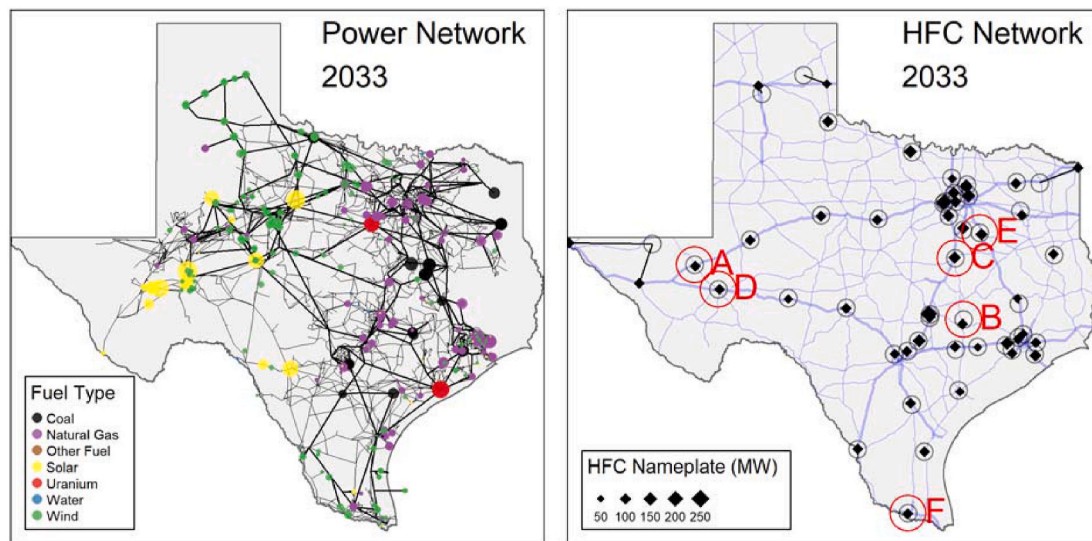


Fig. 2. Modeled system topologies. **Left:** Modeled power generation and transmission network. Sizes of circles and thicknesses of lines represent the nameplate capacities and power transfer limits of generators and power lines, respectively. To note are the large concentrations of solar resource in the west, and of wind resource in the north. **Right:** Modeled location and peak power demand of HFC stations (black diamonds) on the highways (blue lines), along with the feeder lines (black lines) that interconnect them to the nearest transmission load bus (gray rings). The red circled stations are especially impactful on the power system and are referenced in the results. Slow-charging and residential infrastructure are also modeled but omitted from the figure. (For interpretation of the references to color in this figure legend, the reader is referred to the Web version of this article.)

demand profile as per data available from The EV Project (INL, 2013). (See Fig. 3, left side.) The HFC network is the focus of this study and is modeled in more detail: the location of each station is based on the Tesla Supercharger network as it is operating or under construction in Texas in 2020. There are 48 such Supercharger stations, representing about 425 individual fast-chargers and 65 MW of total rated power capacity (Github, 2020). We choose not to incorporate infrastructure from other HFC developers because the Tesla network is well represented along major highways in Texas and because HFC counts and distributions will be manipulated in our analysis as sensitivities. Each modeled HFC is connected directly to the transmission system via the nearest load bus. The HFCs and their grid connections are shown in the right panel of Fig. 2.

Demand profiles for the HFCs are also derived from The EV Project data (INL, 2013). We applied a sampling algorithm to generate realistic demand variation, fitting normal distributions to the quantile data available from INL for each 15-min interval, and for each hour and each charger sampling from the appropriate distribution (top right of Fig. 3). The individual charger demand profiles are summed at each station to create a station-level demand to be served by the power grid (bottom right of Fig. 3). The aggregate demand from an HFC station in a given hour is thus an averaged view of demand for that hour across an entire year: busy travel days and slow travel days cannot be modeled with this methodology, and so peak stresses on the grid are underestimated. These demand profiles are also static in the simulations: both residential and HFC demand are inflexible in the zero-mitigation scenarios. This is an important assumed feature of highway charging behavior, although we explore price-responsive demand as one potential mitigation strategy.

We extrapolate the HFC network to 2033 by rescaling the sizes of existing HFC stations.⁴ The LTSA projects 3 million passenger EVs on Texas roads by 2033 with a peak charging demand⁵ of 6 GW. Using empirical data of many countries' currently deployed EV charging networks (IEA, 2019), we estimate linear models that relate (1) the number of chargers (slow and fast) to the number of passenger EVs on the road, and (2) the number of fast-chargers to the number of all chargers. With both relationships, we convert the 3 million forecasted EVs for 2033 to 34,000 fast-chargers and 300,000 slow-chargers and assume standard power ratings of chargers: 150 kW for a fast-charger and 20 kW for a slow-charger (Lee and Clark, 2018). Applying the median INL utilization curves (Fig. 3) to the slow-chargers recovers the LTSA's 6 GW peak demand prediction, with a mean hourly value of 3 GW. This incremental slow-charging load is distributed through our modeled power system the same way as the initial slow-charging load: pro-rata according to individual load-bus power ratings. Sampling from the INL curves to determine HFC load predicts an incremental peak demand of 1.6 GW and a mean hourly demand of 700 MW from a total nameplate capacity of 6 GW. The incremental HFC load is distributed pro-rata among existing Tesla Supercharging sites according to present charger counts.

During our analysis we define the above configuration as the "LTSA EV Penetration" scenario. We also evaluate lower and higher penetration configurations based on 50%, 75%, 125%, and 150% of the forecasted number of EVs on the road, respectively, as the LTSA forecasts.

2.4. Production cost modeling (PCM)

To simulate the operations of the power grid we use a commercial

⁴ Although it is certain that more charging locations will be developed by 2033, they will probably be clustered like the gas stations that exist along highways. Since clusters will connect to the same point on the transmission network, the impact on the power system of few very large stations as we model would approximate that from a cluster of many smaller stations. See Section 4.1 for more discussion of proactive HFC siting as a mitigant.

⁵ The LTSA does not distinguish between slow- and fast-charging. For context, there were 8 million new private automobile registrations in Texas in 2017 (US FHA, 2017).

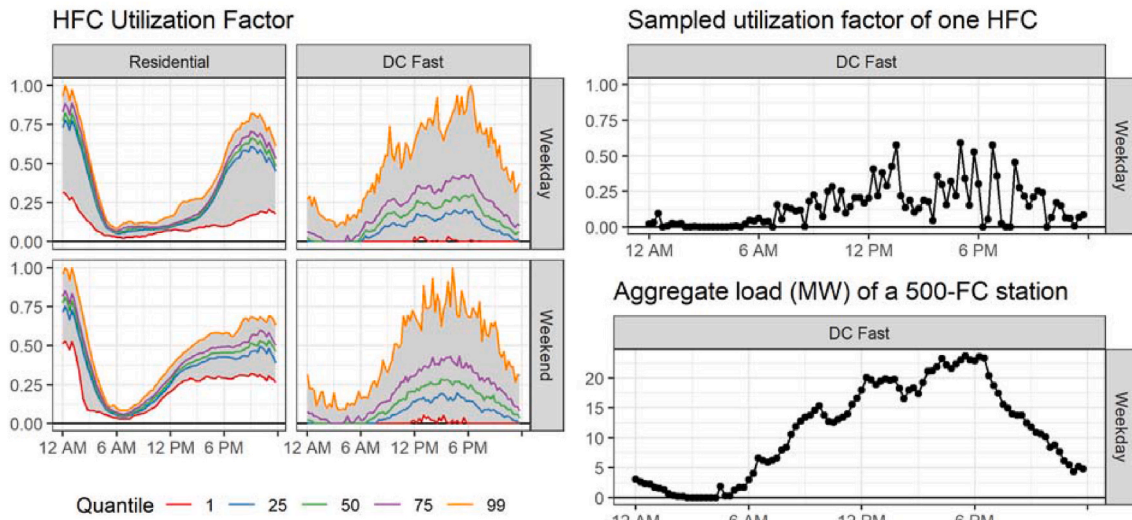


Fig. 3. EV charger demand profile simulation. Left: Empirical results from The EV Project (INL, 2013) showing hourly utilization factor distributions for 100 publicly accessible DC fast-chargers (analogous to our HFCs) and the 6474 private residential Level 2 chargers that were tracked over the course of 2013. **Top right:** We fit normal distributions to each 15-min interval of the FC data, from which we sample during scenario construction to represent individual charger demand. **Bottom right:** Station-level demand for HFCs is the summation of many individually sampled demand profiles, here 500.

grade PCM, the Polaris Power System Optimizer (PSO) that is implemented on the AIMMS optimization platform and solved using CPLEX, to simulate the day-ahead power market in ERCOT. PSO implements the commitment and security-constrained economic dispatch problem with the linearized (“DC”) power flow approximation. PSO has been showcased at FERC technical conferences (Tuohy et al., 2013; Goldis et al.,

schedules at the sub-hourly time scale (Burnham et al., 2017). Our model does not capture these costs.

The relevant outputs from the PSO model include operational metrics like hourly generation dispatch and curtailment, transmission line flows, and fuel consumption; financial outcomes like nodal prices (LMPs) that include energy, congestion, and loss components, generator

$$\text{Cost} = \underbrace{\sum_h (\text{Variable generation costs} + \text{Fixed generation costs} + \text{Net Storage Costs})_h}_{\text{Economic Costs}} + \underbrace{\sum_h (\text{Unserved energy penalties} + \text{Transmission limit penalties} + \dots)_h}_{\text{Penalty Costs}} + \text{all simulation hours, } h \tag{1}$$

2014), used in academic work (Tabors, 2016; Goldis, 2015), and served as a benchmark for the development of other PCMs, such as Sandia National Laboratory’s Prescient PCM (Siirola, 2018).

We configure PSO with a simplified set of market rules that ease the interpretation of results as shown in Table 1. The first five assumptions are conservative in the sense that they likely underestimate the system costs of serving HFCs. Since HFC demand profiles are volatile, they place a burden on real-world grid operators for procuring fast-response reserves to deal with real-time deviations from expected day-ahead

revenues, and cost to load; and the shadow prices for model constraints and the final objective function value. The objective function value (hereafter “cost”) is particularly important as it represents one annual operational cost number for each of our modeled scenarios. It is calculated according to Equation (1) below. The solution cost decomposes into the “Economic Costs” from generation operation and redispatch as well as the “Penalty Costs” from the violation of system constraints.⁶ Although there are many system constraints embedded in the model that could trigger penalty costs, only transmission line penalties are incurred during our simulations. The Economic and Penalty dichotomy is important for our interpretation of our results: while the penalty costs are figmentary in the sense that they represent unrealistic system operations, they nevertheless capture the costs of serving incremental infrastructure. The alternative modeling technique would be to value unserved demand from HFCs and avoid transmission penalties. Instead we allow HFC demand to violate feeder transmission line limits since those violations have a well-defined value from grid operators (Potomac, 2020).

While the PCM is configured as above based on grid operator practices today, we expect it will maintain its validity through 2033 and

Table 1

PCM Assumptions. The transmission penalty is derived from ERCOT market rules (Potomac, 2020), while the unserved energy penalty is set above ERCOT’s \$9000/MW offer cap (Brattle, 2019a) to ensure that the least-cost optimization model prioritizes serving load to the extent possible, even if it means violating one or more transmission constraints.

(1) Energy-only (no ancillary services or capacity payments are modeled)	(4) Hourly resolution
(2) Day-ahead only (no recommitment or redispatch in a real-time market) with hourly resolution	(5) Rolling-horizon approach with a 24-h simulation period informed by a 36-h look-ahead planning period
(3) Deterministic realizations (no uncertainty about load or generation requiring conservative commitment)	(6) \$15000/MW penalty for unserved energy and \$9251/MW penalty for transmission limit violation each hour

⁶ Additional penalty terms are omitted to save space. They are uniformly zero in all of our simulations.

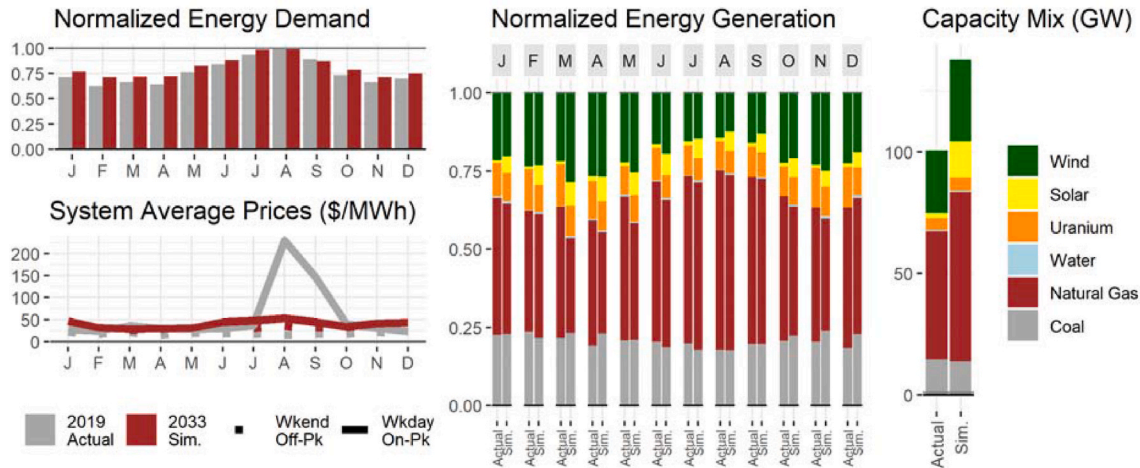


Fig. 4. Comparison of simulated ERCOT system in 2033 to actual ERCOT system in 2019. **Top left, Load:** Total monthly energy consumed in the ERCOT footprint, normalized by the load of the highest-consumption month. **Bottom left, Prices:** Average system prices paid by load per month, for two representative shapes: the highest-load shape, weekday “on-peak” hours (6AM–10PM), and the lowest load shape, weekend “off-peak” hours (10PM to 6AM). The simulated data are the load-weighted averages of ERCOT weather zone LMPs. The historical data are the load-weighted averages of DA ERCOT load zone SPPs (LMP + reserve costs). Differences in the summer months may be due to unmodeled reserve costs or transmission gold-plating, as previously noted. **Center, Generation:** Monthly energy produced in the ERCOT footprint, segmented by fuel type, and normalized by total monthly generation. **Right, Installed Capacity:** Total system power capacity, segmented by fuel type. (For interpretation of the references to color in this figure legend, the reader is referred to the Web version of this article.)

beyond, including the high penalties for transmission constraint violation and unserved energy. Even if grid operators were to be majorly restructured, the PCM configuration represents efficient economic dispatch which should remain the targeted outcome (Hogan, 2014).

2.5. Validation

To validate the many assumptions used in defining the PCM for this study, we performed a benchmark test of our Base Case (the 2033 coupled charger-grid model without HFCs) against actual ERCOT operations in 2019 (Github, 2020). We compared monthly energy demand, monthly power prices (system averages), and monthly generation by fuel type, as shown in Fig. 4. The demand and generation were compared on a normalized basis given the significant growth of both in absolute terms from 2019 to 2033. We found good matching between the two systems, specifically noting: load patterns with peaks in the summer and winter (5.1% mean absolute error of monthly normalized loads) and seasonally-dependent generation shares for different technologies (2.7% mean absolute error of month-fuel normalized generation).

3. Results and discussion

We present our basic results in Section 3.1, showing how the aggregate system cost increases due to HFC power demand in various EV penetration scenarios. We also discuss how these costs are decomposed between Local vs. Zonal Effects and Economic vs. Penalty components, and we make use of the granular resolution of our model to investigate the impacts due to individual HFC stations. In Section 3.2 we make use of this framework to show how mitigation methods, and in particular energy storage and demand flexibility, affect these results. Section 3.3 generalizes these findings in a discussion.

3.1. Incremental costs due to HFCs

Fig. 5 shows the incremental power system costs by month due to the HFC network across different EV penetration levels (and corresponding HFC power demands). The incremental costs are decomposed into the difference in the modeled system cost between the Distributed Case and the Base Case (“Zonal Effects”) and between the Concentrated Case and the Distributed Case (“Local Effects”) as introduced in Fig. 1 and into

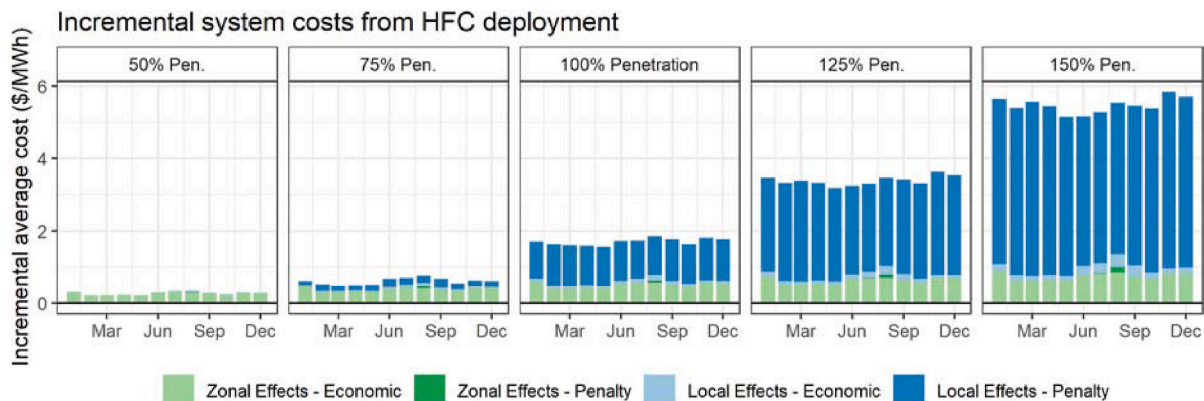


Fig. 5. System cost impacts of HFCs. Incremental system costs of HFC infrastructure are measured as the difference in objective function value between Cases, normalized by Base Case load. the Base, Distributed, and Concentrated Cases, for various levels of EV penetration relative to ERCOT’s LTSA forecasts for 2033. Key trends are the increasing costs with increasing EV penetration, the presence of both Local and Zonal Effects, and non-linearity in the Local Effects.

Economic and Penalty Costs as introduced in Equation (1). The costs are normalized by the total system load (excluding HFCs) in the LTSA EV Penetration Base Case for each month.

We describe three effects in Fig. 5. First, the additional demand from HFCs increases costs, and this effect increases as EV penetration increases. This is expected, since additional HFCs are incremental load to be served by incremental generation. In the 100% Penetration scenario, the average annual costs increase by \$1.70 per MWh of load served. This corresponds to 3%–6% of simulated system-wide monthly-averaged LMPs (shown in Fig. 4, ranging from \$27/MWh to \$53/MWh), or about 8% of the average annual Base Case system costs (i.e., the system without any FC demand, about \$21 per MWh of load served). Second, all four cost types – Penalty and Economic components of Local and Zonal Effects – are present, and the magnitudes of Local and Zonal Effects are similar in the baseline LTSA EV Penetration configuration. Third, the costs increase nonlinearly with EV penetration due to rapidly growing Local Penalty Costs. (For example, first differences of July total cost increases as EV penetration grows in steps of 25% are \$0.36/MWh, \$1.05/MWh, \$1.55/MWh, \$1.99/MWh.) The other components grow more slowly and linearly. This reflects a discontinuity in marginal operational cost as EV penetration increases: as soon as an HFC station grows large enough to cause network congestion or thermal violations in its vicinity, it becomes much more expensive to operate. This assertion is supported by Figure A4 in the Appendix, which shows how certain HFC stations rapidly become more impactful to system costs as EV penetration increases.

We further explore the Local Effect components in Fig. 6. We plot distributions of the absolute values of the difference of hourly LMPs, hour by hour, between the Distributed Case and the Concentrated Case across the full year for each HFC station, restricting the analysis to the LTSA EV Penetration case. (By choosing the Distributed Case as a baseline, we exclude effects from aggregate differences in demand.) These distributions of differences are indicative of the local impacts attributable to each individual HFC station. Because of the interconnectedness of the grid, such a proxy for individual effects must be used. The main features of these results are (1) the large range of local impacts across HFC stations – the means span five orders of magnitude from about \$1/MWh to about \$10,000/MWh – and (2) that the majority of HFC stations have relatively low impact at about the \$1/MWh level; the majority of system impacts is caused by a minority of HFC stations. At these exceptionally impactful stations we observe bimodal distributions in the difference in LMPs, shown by the violins in the right panel of Fig. 6. The high-end mode is indicative of periodic congestion events

that elevate LMPs in the Concentrated Case over the Distributed Case, while the low-end mode (where there is little difference between cases) indicates low load periods. The right-hand panel of Fig. 6 also highlights that the impacts do not scale simply with HFC peak power demand.

3.2. Mitigation of increased system costs

We simulate two strategies to mitigate the increased system operation costs from HFC stations shown in the previous section. We consider both (1) the installation of co-located energy storage and (2) the implementation of demand flexibility programs as feasible strategies that HFC station developers might consider. Energy storage is modeled as a grid-connected 4-h battery with specifications based on the Tesla Powerpack; we assume constant 89.5% round-trip efficiency, 100% depth of discharge, and no degradation with use (Tesla, 2020). Since the battery is assumed to be co-located with the HFC station, it is modeled on the same node in the power system. In every other respect, we model storage as a fully independent wholesale asset that is optimized by the PCM in the same way as other generation: to provide least-cost system operation. Finally, we only model energy storage at the six labeled HFC stations in Fig. 6, chosen as particularly likely to require mitigation efforts.

The modeled demand flexibility allows an individual HFC's charging demand to be shifted forward or backward in time by 1 h, without expense, in response to wholesale prices. This relaxes an important assumption, that HFC demand is inflexible (Burnham et al., 2017). Flexible HFC demand might correspond to an EV driver spending time in a co-located café or co-working space while waiting for lower charging rates. We take a recursive approach to add flexibility to our relatively static modeling framework, instantiating new model configurations with reference to already solved models. We represent flexibility in increments of 5% of the maximum demand of each HFC. As an example, to simulate new HFC charging profiles with 5% demand flexibility, we reassign demand from the base charging profile (with 0% flexibility, Fig. 3) by referencing prices from an already solved model with 0% demand flexibility; then to simulate charging profiles with 10% demand flexibility, we reassign demand from the 5% demand flexibility charging profile using the prices from the already solved model with 5% demand flexibility; and so on. This process and its results are shown visually in Figure A2 in the Appendix.

Fig. 7 shows the mitigation that these strategies provide as their level of implementation in the system increases and as the level of EV penetration in the system changes. Here again we focus only on the Local

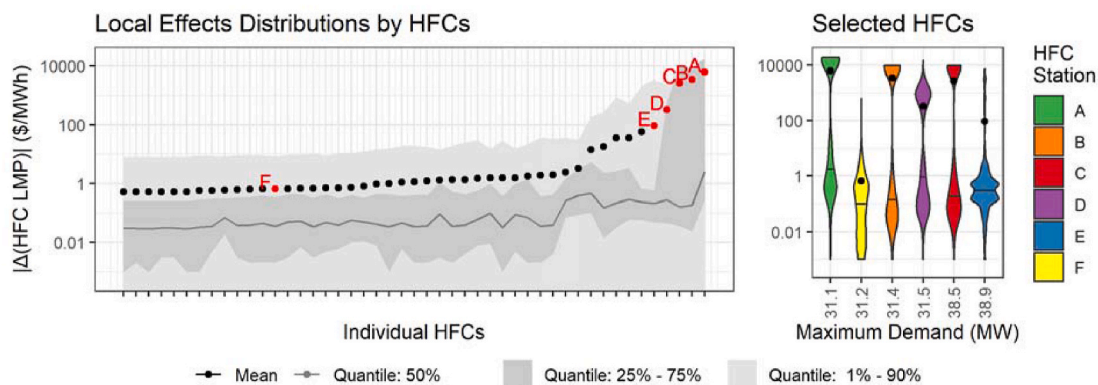


Fig. 6. Variation in local effects by HFC station. Left: Distributions of hourly charging impacts from HFCs, with each HFC station arranged on the x-axis in order of mean local impacts. The plotted distributions are the differences in absolute hourly LMPs between the Concentrated Case and the Distributed Case. Red dots indicate the selected HFC stations on the right-hand side. Right: The five most impactful HFC stations, with average effects from Local Constraints \geq \$100/MWh, and a selected normal HFC station (F) are plotted. These stations are highlighted in Fig. 2 above. The stations are arranged from left to right in order of ascending peak demand, illustrating that impacts do not correlated simply with size. (For interpretation of the references to color in this figure legend, the reader is referred to the Web version of this article.)

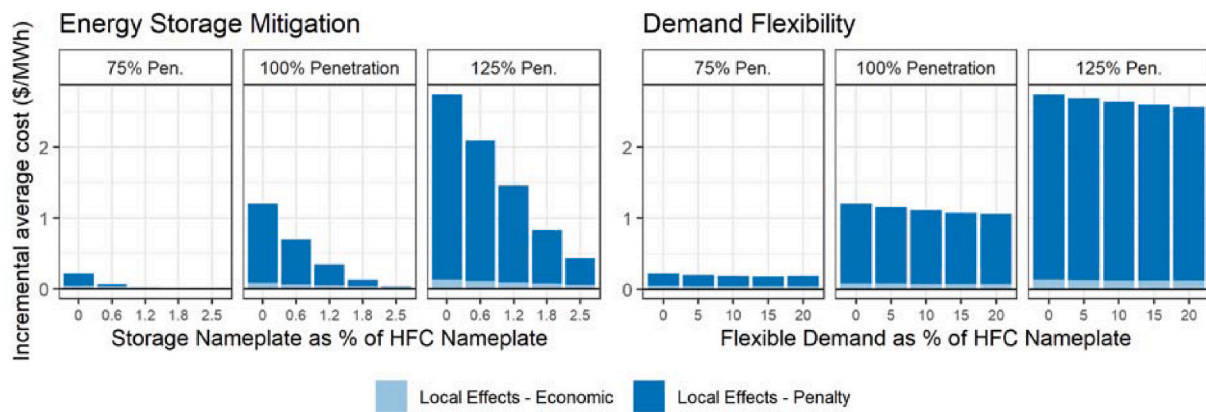


Fig. 7. Effectiveness of strategies to mitigate HFC deployment. The y-axis plots the increase in system objective function from the Distributed Case to the Concentrated Case (thus showing the “Local Effects”) with a variable amount of mitigation (modeled only in the Concentrated Case). The x-axis shows the variation in the amount of mitigation deployed, represented as a percentage of modeled HFC nameplate capacity in the system. The “100% Penetration” case is the LTSA planned EV penetration level.

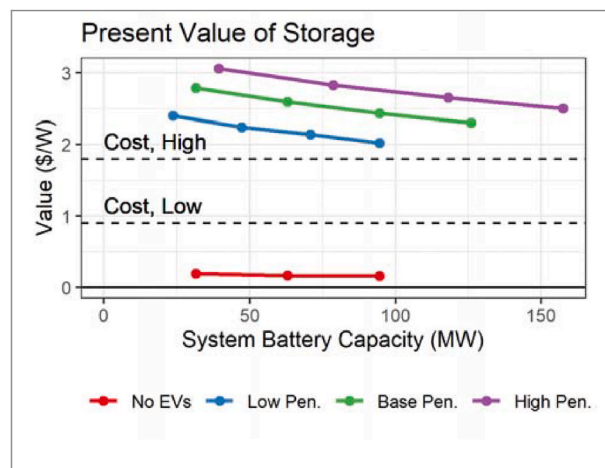


Fig. 8. Present value of storage as a function of EV penetration. The present value of battery storage (normalized by battery nameplate capacity) is plotted against battery capacity for different cases of EV penetration. Battery value here means positive value to the power system, as measured by the change in the economic component of the objective function value from the Concentrated Case without batteries to the Concentrated Case with a variable amount of batteries. Two estimates of the present value of wholesale energy storage costs are superimposed for reference, which correspond to a range of \$225/kWh-\$469/kWh for capital costs given by Lazard (2019) for 4-h wholesale batteries operational. Fig. 8 shows the results of this exercise for simultaneous deployment of energy storage at the 6 most impacted HFCs in our simulation, those highlighted in Fig. 2. The figure shows that the marginal benefit of the battery decreases as its size increases, a trend consistent with prior studies evaluating the value of storage (Mallapragada et al., 2020), due to increasingly active management of high-priced hours. Despite this, the batteries are still profitable investments in all tested EV penetration scenarios that contain HFCs. The co-located batteries are uneconomic, however, in the simulations that do not contain HFCs. (Operational batteries exist at the HFC nodes though HFC stations are not present.)

Effects but with a twist: incremental system costs from the inclusion of HFCs are shown on the y-axis, measured as the additional cost of the Concentrated Case with mitigation measures over the Distributed Case without mitigation measures. Thus we effectively ask how much of the Local Effects due to HFCs a specific mitigation measure is able to mitigate; an incremental cost of zero would indicate that the mitigation strategy mitigated all of the Local Effects of the HFC station. As before, we decompose the Local Effects into Economic and Penalty components. Fig. 7 shows that both energy storage and demand flexibility mitigate the system cost impacts of concentrated HFC demand, primarily by reducing Penalty components of Local Effects, but energy storage is much more effective: storage deployed at only 0.6% of the nameplate capacity of all HFC stations on the system outperforms demand flexibility deployed at 20% of nameplate capacity. (It should be recalled, however, that the storage is concentrated at the 6 most impacted nodes,

while demand flexibility is applied across all HFC stations.)

The reason for this difference is intuitive if demand flexibility is considered as a highly constrained (but cheap) 1-h battery. This is close to the truth: a given unit of flexible demand is assumed to be able to transpose itself either 1 h into the past or the future, to times $t-1$ or $t+1$, depending upon the power grid’s LMP price signal, just like a battery performing energy arbitrage. This is more constrained than true storage, though, which may carry its charge for a functionally unlimited amount of time and also discharge over a longer period of time. Understood this way, both mitigation strategies work by shifting grid electricity consumption at HFCs during grid-strained periods. The 4-h battery, though, can mitigate longer strain on the grid and so is more effective at managing congestion introduced by grid-HFC interactions, which lasts for multiple hours (see Figure A3 in the Appendix).

3.3. The importance of locational and temporal characteristics of charging demand

Where a particular HFC station is located is a crucial determinant to its overall operational impact on the power grid. This is an implication of the distributions shown in Fig. 6, which on the left shows the extreme variation in system impacts between stations and on the right show that these impacts, where they occur, are not correlated with the size of the station's demand. Additionally, the locations of these stations, highlighted in Fig. 2, do not reveal any obvious geographic patterns. Rather, our model demonstrates that the impacts depend upon the relative strength of the transmission grid in each HFC station's locality. (This point is illustrated in Figure A1 in the Appendix, which shows an example of how a local network with low power transfer limits can restrict an HFC station's operations.) This insight around "hosting capacity" is not novel. Just as the literature surrounding distribution network-scale impacts of EV chargers is concerned with peak usage overwhelming network components, the same holds true for HFCs integrated directly into the transmission network. Not all 69 kV feeder lines on the power grid are sized to serve the incremental 10MW–100MW peak loads that the simulated HFC stations represent.

What we have newly demonstrated, however, is that *which* HFCs will cause problems *when* does not follow a predictable pattern. It is not geography or peak demand alone that determine these, but the combination measured against local conditions, which is not obvious from a casual survey. So long as the charging load at an HFC station is reliably servable by its neighborhood transmission lines, its costs to power grid operation will only be mild: the incremental load will result in more generation being dispatched from the top of the generation supply stack. These incremental economic cost components, shown as the lighter colors in Fig. 5, are approximately smooth functions of the incremental load in large power systems. As HFC station size increases past the capacity of its feeder network, however, its usage may threaten to violate system constraints, and so congestion begins to much more severely impact power grid operational costs. These severe impacts are represented as the penalty cost components in our model. Fig. 5 shows these costs increasing non-linearly as EV penetration increases on the system: with each penetration step, more of the HFC stations breach the practical limit of their surrounding network to meet their demand, and so penalty costs appear. The point at which penalty costs appear for a given HFC depends on its demand and the ability of the local network to meet it; these points vary substantially across the system. The ability to estimate the full cost of HFC integration thus depends on the ability to exactly situate and simulate HFC stations on the power grid. A zonal simulation model, of the type used in large scale charger-grid coupling studies (such the studies by Heuberger et al. (2020) and Szinai et al. (2020) described in the Introduction) will only capture the Zonal Effects of integration, which are roughly 50% of the total effects in the LTSA Base Penetration case for 2033, as shown in Fig. 5.

Just as important as the location of an HFC station for determining its effect on power system operational costs is the temporal nature of its demand, i.e. the charging profile, overlaid on pre-existing system load. This study uses the aggregate charging profiles shown in Fig. 3, which for HFCs show an important characteristic: they have relatively wide peaks. The proportion of time on a median day that the charging profile is above 50% of its daily peak is roughly 8 h. Since the peak demand period is when the HFC will most strain the power grid, the duration of its peak is important. If the broad peak in HFC charging demand observed in the limited empirical data holds true even with increasing adoption of EVs, it has the potential to drive congestion events and high-priced periods that far-exceed the capabilities of a 1-h battery and even a 4-h battery to shift (See Figure A3 in the Appendix for additional

illustration of congestion durations at HFCs.). While it follows that longer duration batteries would be more effective mitigants, diminishing returns should be expected, and longer duration storage solutions are accompanied by increasing costs that must be weighed against their benefits.

4. Conclusions and policy implications

4.1. Roles for mitigation strategies

As a case study, we consider the economic cost-benefit problem confronting the developer of an HFC station who wishes to co-locate (or is required by the system operator to include) a 4-h battery to mitigate local system impacts. Since the battery will be grid-connected, it is able to profit-maximize and monetize more benefits than if it were constrained only to offset the cost increases associated with the relevant HFC station. While we could simply recover the revenue accorded to the battery in the PCM solution – its optimal energy arbitrage value – we consider a more optimistic case wherein the developer is working together with the local utility or grid operator and is able to capture more of the economic benefits via bilateral transfer payments. Thus we model the Economic components of the system-wide mitigation value from the battery as its value or revenue (See Fig. 5. Note that also including the Penalty components of our results is not necessary to make our point.). Under this model, we can calculate the present value (PV) of the battery system's revenues for a 15-year lifetime with a 7% discount rate and compare it against the PV of the battery system's lifetime costs, both capital and.

The above simplified illustration of the investment decision for 4-h batteries at HFC stations is presented to motivate two points. First, just as the locational characteristics of the HFC load are critical to determining station operational impact on the power grid, the location of mitigation infrastructure is also critical. It is only once strong LMP effects are caused by charging demand that energy storage can break even on its costs via energy arbitrage value. Second, although privately developed batteries that profit from the energy market can make financial sense, Fig. 8 points to diminishing returns as the trendlines run to the right: the grid will not support an unlimited amount of profitable installed battery capacity. Considering that the 2033 ERCOT system will almost certainly host several hundred MW or more of grid-tied energy storage, and with 100 MW already in operation by 2019, the economic case for future HFC co-located storage may be weaker than implied here (EIA, 2020b). (The, 2018 LTSA does not forecast energy storage in any of its analytical cases, which is why we do not model it in our Base Case.)

Another potential mitigation strategy beyond energy storage and demand flexibility is transmission reinforcement, either through reconductoring to increase the power transfer limits of existing lines or through the construction of new lines. In light of the above discussion, it is natural to think of expanded transmission capacity as another technology capable of shifting demand: it is an "infinite duration battery" that relies on dispatchable generation elsewhere in the grid and for a fixed nameplate capacity will be at least as effective as storage or flexibility. A significant new degree of freedom is introduced when considering transmission expansion, however: the system planner must choose *which* of the local transmission lines to upgrade, or *where* to construct a new one. For energy storage and demand flexibility, the planner must only decide how large of a system to co-locate with the HFC station. (It is granted that energy storage and other flexibility resources can be added anywhere on the power grid, but this paper takes the mitigation strategies from the perspective of the developer, who will be much more practically constrained to the locale of the HFC station.) For these reasons of added complexity, we did not systematically

analyze transmission upgrades. We are able to use our model to explore case studies, however, as shown in [Figure A1](#) in the Appendix.

While demand flexibility could be considered an inherent (if limited) mitigation measure, and energy storage and transmission reinforcement as reactive measures, there also exists the possibility for cost mitigation and avoidance through proactive siting of HFC stations. Such siting would cause the stations to be built in low-impact locations with strong grid connections. This is an active area of research with immediate implications as governments and firms plan charging network investments. The problem formulation in such studies usually does not consider minimizing power system costs, but instead seeks to minimize driver range anxiety and total power rating of EV chargers installed (For example, [Xu et al. \(2020\)](#) recently estimated an optimal charging network topology on the Texas highway system. [Erbaş et al. \(2018\)](#) did the same for Turkey. Neither of these studies accounts for power system operational costs.). Particularly if government or utility policies were reformed to shift grid costs to EV charger developers, however, it is likely that “optimal” locations would shift to reduce costs in the power system. Although we did not attempt to co-optimize the location and operation of the EV charging infrastructure in this study, we do note that moving HFC stations even by tens of miles will not always change the point of interconnection (See [Figure A5.](#)), especially in rural areas, owing to the limited number of transmission interconnection points. Therefore, the practicality of proactive siting as a mitigation method for transmission-level costs is not immediately apparent.

We return the discussion to transmission reinforcement and energy storage co-location as effective mitigation strategies that do not break the inflexibility assumption for HFC demand. They are both important options for system operators and private developers to consider, but they differ in key ways. Transmission lines are commonly more highly regulated assets than energy storage facilities, and the latter may have difficulty finding approval for utility rate base decisions ([Pandžić et al., 2018](#)). In the USA, recent market reforms brought on by FERC Orders 841 and 2222 promise to promote the merchant development of storage, while FERC Order 1000, which attempted to do the same for transmission, has seen mixed success ([Brattle, 2019b](#)). Both transmission line reconductoring and new-build costs scale by length and capacity whereas energy storage costs scale by duration and capacity. Transmission construction has longer lead times than storage development ([Eto, 2016](#); [EIA, 2020b](#)). These factors combine to make the choice of mitigation measure complex, even after the need for mitigation is identified, which the rest of this paper shows to be no easy task itself.

4.2. Conclusion

Projections for EV adoption continue to be revised upward, which makes studying the impact of this new type of demand on the power system increasingly important. We complement existing studies of the impact of EV charging demand on the power grid (1) by using a spatially and temporally resolved PCM of the transmission-level power system, and (2) by focusing specifically on highway fast-charging infrastructure, which is unique in the inflexible, high power, and spatially concentrated nature of its power consumption. Through simulations, we quantify the cost impacts of transmission congestion and generation redispatch attributable to HFC deployment, and we show that these impacts are irregularly distributed according to the specific network location of the fast-charging HFC station and the temporal nature of fast-charging demand. By segmenting and attributing the incremental power system costs due to HFC integration, we demonstrate that the temporal and spatial resolution of our model is necessary to fully account for these costs. We further show that these impacts can be mitigated, but that such mitigation must account for both the locational and temporal aspects of the problem. Such aspects advantage longer-duration solutions, such as energy-storage, over shorter-duration solutions, such as demand flexibility.

While compelling, our results could be further developed. A simple but powerful extension of our analysis would be to model more commercial details in the PCM. Accounting for real-time markets, ancillary services, and non-deterministic load and weather outcomes could demonstrate higher costs for HFC integration as well as more benefits from mitigation. A more involved extension would deepen our mitigation analysis by systematically analyzing transmission solutions, as well as battery storage degradation costs. More novel grid management techniques, such as the temporary relaxation of voltage constraints, could be explored ([Cvijić et al. \(2018\)](#) have proposed AC power flow models to investigate this.). Looking to the transportation side of our model, implementing a dynamic representation of HFC demand, such as [Szinai et al.'s \(2020\)](#) BEAM behavioral model, would add more nuance to our results and allow us to investigate peak grid impacts, e.g. around heavy-traffic holidays. Short of full behavioral model coupling, a more detailed but still exogenous charging model could be integrated, such as that developed by [Dominguez-Jimenez et al. \(2020\)](#). Mitigation methods might also be considered inside the transportation model that could relax the inflexibility assumption of HFC demand. For example, dynamic tolling on highways could reroute traffic around grid congestion, or drivers' flexibility could be increased by giving them access to pricing information *before* they leave on a journey. Extending our study in these directions ultimately would allow us to better investigate the total economic cost-benefit of HFCs. In turn, that would make discussion of different models for deploying HFCs – e.g. private developer driven, utility driven, etc. – compelling. This research might also be generalized to consider more broadly the effects of electrification: we have shown that the inflexibility assumption from HFCs is important to the cost and mitigation analysis, and this may hold for other new types of electricity demand as well. We have also shown how a “duration framework” helps to understand the substitutability of demand flexibility, energy storage, and transmission reinforcement for mitigation. This viewpoint might transfer to other applications as well.

The results of this research should help to persuade system operators and utilities to begin studying HFC integration challenges to prevent operational difficulties from arising that would prevent a slowdown in EV charging infrastructure buildout. A proactive approach would identify likely concentrations of HFC stations along transportation corridors and stress test the local transmission infrastructure, as we have done here. The increasingly interwoven systems of power and transportation must be kept in close coordination.

CRedit authorship contribution statement

Andrew M. Mowry: Conceptualization, Methodology, Data curation, Formal analysis, Visualization, Writing – original draft, Writing – review & editing. **Dharik S. Mallapragada:** Conceptualization, Methodology, Administration, Writing – review & editing.

Declaration of competing interest

The authors declare the following financial interests/personal relationships which may be considered as potential competing interests:

Andrew Mowry was employed by Ørsted A/S, a global renewable energy infrastructure developer, at the time of article submission. That relationship did not influence the conception or execution of this research, which formed part of Andrew Mowry's master's thesis at MIT.

Acknowledgements

The authors acknowledge Patrick R. Brown for his helpful comments on the analysis, and also Francis O'Sullivan and Christopher Knittel for initiating discussion and research of this topic. The authors acknowledge funding support from the Low-Carbon Energy Center on Electric Power Systems at the MIT Energy Initiative.

Appendix

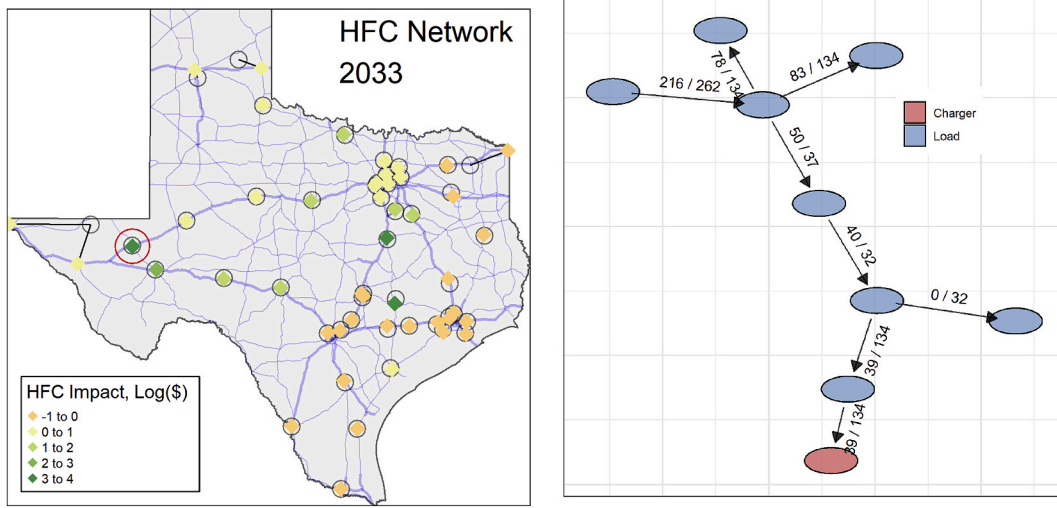


Fig. A1. Example local network topology. Left: An illustration, similar to the right side of Fig. 2, depicting the modeled HFC stations colored according to their impacts on the system. This impact is measured as the logarithm of the absolute difference between the HFC nodal LMPs in the Concentrated Case and the Base Case, using the Base EV Penetration from ERCOT’s LTSA. This is the same metric used in Fig. 6. Right: The local network topology at the circled HFC station in the left panel. The edge annotations represent the power transfer (MW) along each line as a fraction of that line’s rated line limit (MW), for hour ending 6PM on August 21st in the model. **Comment:** The left panel emphasizes that the most impacted HFC stations are geographically distributed, and, together with Fig. 6, imply that the cause of individual HFC station impacts is local network congestion. The right panel illustrates power transfer bottlenecks that may occur to supply power to HFC stations.

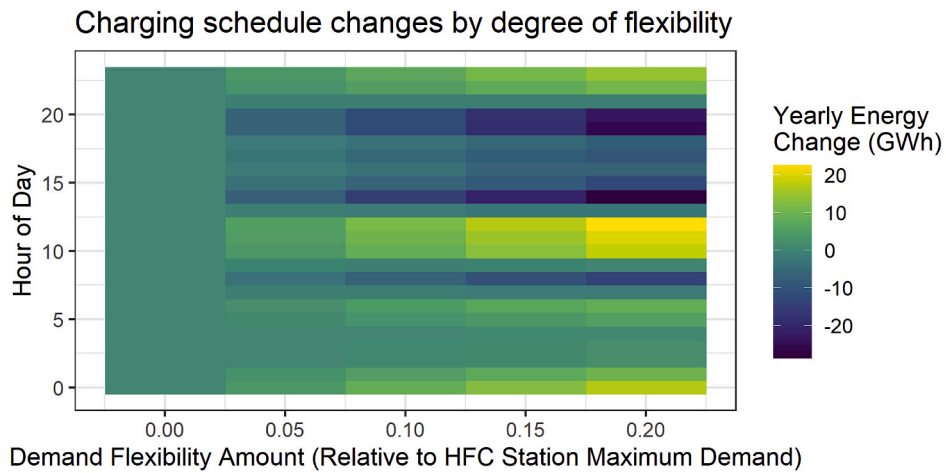


Fig. A2. Modeling demand flexibility. Here we show how hourly charging schedules shift as the HFC inflexibility assumption is relaxed. The color in each tile corresponds to the system-wide charging demand in a specific hour, summed over the entire year, and differenced against the (inflexible) base case. As the amount of modeled (1-h) demand flexibility increases from 0% to 20% of the maximum demand of each HFC station, aggregate charging activity at modeled HFC stations shifts predominantly from the mid-afternoon to the late-morning and late-night periods.

Characteristic congestion event durations at HFC stations

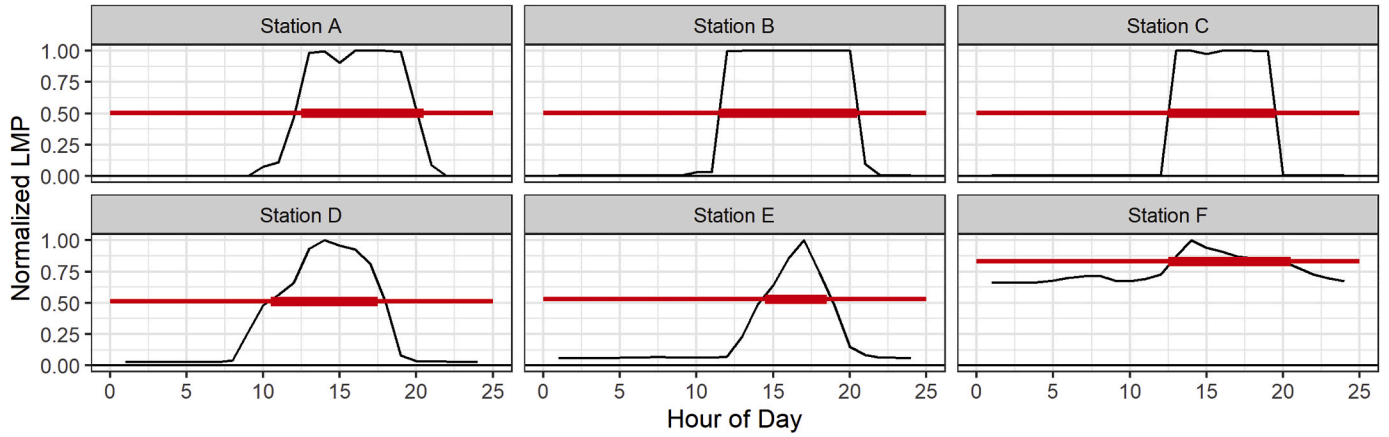


Fig. A3. Congestion duration. The normalized hourly LMPs, averaged across all simulated days, at six high-impact HFC stations are plotted in black for the Concentrated Case without any mitigation. The bolded red lines illustrate the “full width at half maximum” for each of the HFC station price curves. This visually illustrates the different durations of congestion events (high priced time periods) at different HFC stations. The referenced HFC stations correspond to those highlighted in Figs. 2 and 6.

Most Impactful HFC Stations By Scenario

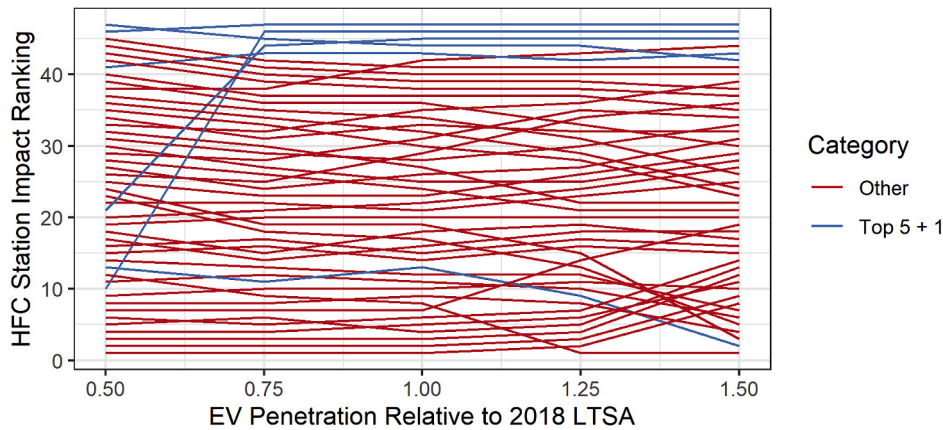


Fig. A4. Most Impacts HFC Stations by Penetration Scenario. Here we show the relative impact that each HFC station has on the power grid, as measured by the difference in mean absolute hourly LMPs at each HFC station’s node between the Concentrated Case and the Distributed Case, which is the same methodology used to present the data in Fig. 6. Higher ranked stations have a higher difference in prices, implying that the stations have more of an impact on the grid. The calculation is done for five EV penetration scenarios, here presented along the x-axis relative to the 2018 LTSA EV penetration scenario. The Top 5 impacted stations as identified in the Main Text (see Fig. 6) for the 100% EV Penetration scenario are not always the top 5.

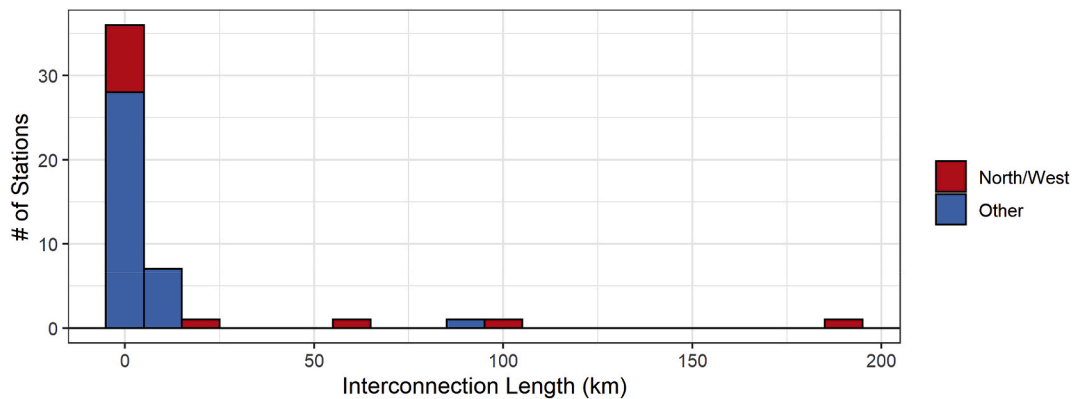


Fig. A5. Distribution of HFC Feeder Line Interconnection Lengths. This histogram shows about 25% of HFC stations we model are at least 5 km distant from their nearest transmission-level bus. For these far-flung stations, there is little ability to optimize power system impacts by moving the HFC stations along the highway networks. Even for the HFC stations closer to their points of interconnection, moving the stations to change the interconnection may not alleviate grid congestion.

References

- Arias-Londoño, A., Montoya, O.D., Grisales-Noreña, L.F., 2020. A chronological literature review of electric vehicle interactions with power distribution systems. *Energies* 13 (3016).
- Autoalliance, 2020. Advanced technology vehicle sales dashboard. Web resource accessed December 2020: <https://autoalliance.org/energy-environment/advanced-technology-vehicle-sales-dashboard/>.
- BNEF, 2019. Electric vehicle outlook 2019. Bloomberg New Energy Finance. Web resource accessed December 2020: <https://bnef.turtl.co/story/evo2019/>.
- Brattle Group, 2019a. Estimation of the market equilibrium and economically optimal reserve margins for the ERCOT region: 2018 update. Web resource accessed December 2020. http://www.ercot.com/content/wcm/lists/167026/2018_12_20_ERCOT_MERM_Report_Final.pdf.
- Brattle Group, 2019b. Cost savings offered by competition in electric transmission. Web resource accessed December 2020. https://brattlefiles.blob.core.windows.net/files/15987_brattle_competitive_transmission_report_final_with_data_tables_04-09-2019.pdf.
- Brown, Abby, Lommele, Stephen, Schayowitz, Alexis, Klotz, Emily, 2020. Electric vehicle charging infrastructure trends from the alternative fueling station locator: first quarter 2020. Web resource accessed December 2020. <https://www.osti.gov/servlets/purl/1665819>.
- Burnham, Andrew, Dufek, Eric J., Stephens, Thomas, Francfort, James, Michelbacher, Christopher, Carlson, Richard B., Zhang, Jiucui, Ram, Vijayagopal, Dias, Fernando, Mohanpurkar, Manish, Don, Scofield, Hardy, Keith, Shirk, Matthew, Hovsapian, Rob, Ahmed, Shabbir, Bloom, Ira, Jansen, Andrew N., Keyser, Matthew, Kreuzer, Cory, Markel, Anthony, Meintz, Andrew, Ahmad, Pesaran, Tanim, Tanvir R., 2017. "Enabling fast charging – infrastructure and economic considerations". *J. Power Sources* 367. <https://doi.org/10.1016/j.jpowsour.2017.06.079>.
- Conroy, Steven, 2020. Tesla energy crisis day 2. Youtube. Web resource accessed December 2020: <https://www.youtube.com/watch?v=k5N2Bo3Zek>.
- Cvijić, S., Ilić, M., Allen, E., Lang, J., 2018. Using extended AC optimal power flow for effective decision making. In: 2018 IEEE PES Innovative Smart Grid Technologies Conference Europe (ISGT-Europe). <https://doi.org/10.1109/ISGTEurope.2018.8571792>.
- Deb, S., Kalita, K., Mahanta, P., 2017. Review of impact of electric vehicle charging station on the power grid. In: 2017 International Conference on Technological Advancements in Power and Energy (TAP Energy). <https://doi.org/10.1109/TAPENERGY.2017.8397215>.
- DOE, 2020. "Electric vehicle registrations by state". Alternative fuels data center. Web resource accessed December 2020: <https://afdc.energy.gov/data/10962>.
- Dominguez-Jimenez, Juan, A., Campillo, Javier E., Montoya, Oscar Danilo, Delahoz, Enrique, Hernández, Jesus C., 2020. Sustainability 12 (18). <https://doi.org/10.3390/su12187769>.
- EIA, 2020a. Annual energy outlook 2020. Web resource accessed December 2020: https://www.eia.gov/outlooks/aeo/tables_ref.php.
- EIA, 2020b. Battery storage in the United States: an update on market trends. Web resource accessed December 2020: https://www.eia.gov/analysis/studies/electricity/batterystorage/pdf/battery_storage.pdf.
- Erbaş, Mehmet, Kabak, Mehmet, Özceylan, Eren, Çetinkaya, Cihan, 2018. Optimal siting of electric vehicle charging stations: a GIS-based fuzzy Multi-Criteria Decision Analysis. *Energy* 163. <https://doi.org/10.1016/j.energy.2018.08.140>.
- ERCOT, 2018. 2018 long-term system Assessment for the ERCOT region. Electric Reliability Council of Texas. Web resource accessed December 2020: http://www.ercot.com/content/wcm/lists/144927/2018_LTSA_Report.pdf.
- ERCOT, 2020. 2020 ERCOT monthly peak demand and energy forecast. Web resource accessed December 2020: http://www.ercot.com/content/wcm/lists/196030/ERCOT_Monthly_Peak_Demand_and_Energy_Forecast_2020_2029.xlsx.
- Eto, Joseph, 2016. Building electric transmission lines: a review of recent transmission projects. Web resource accessed December 2020: <https://emp.lbl.gov/publications/building-electric-transmission-lines>.
- Github (2020). https://github.com/mowryand/HFC_grid_impacts/edit/main/README.md.
- Goldis, Evgeniy, 2015. Topology control algorithms in power systems. Doctoral Thesis at Boston University. Web resource accessed December 2020: <https://open.bu.edu/handle/2144/16306>.
- Goldis, John, Rudkevich, Aleksandr, Tabors, Richard, Omondi, Lorna, 2014. "Use of cloud computing in power market simulations". *FERC technical Conference on increasing real-time and day-ahead market efficiency through improved software*. Web resource accessed December 2020: <https://www.ferc.gov/june-tech-conf/presentations/w1b-3.pdf>.
- Heuberger, Clara F., Bains, Praveen K., Niall Mac Dowell, 2020. The EV-olution of the power system: a spatio-temporal optimisation model to investigate the impact of electric vehicle deployment. *Appl. Energy* 257. <https://doi.org/10.1016/j.apenergy.2019.113715>.
- Hogan, William W., 2014. Electricity market design and efficient pricing: applications for new England and beyond. *Electr. J.* 27 (7) <https://doi.org/10.1016/j.tej.2014.07.009>.
- IEA, 2019. Global EV Outlook 2019: scaling-up the transition to electric mobility. International Energy Agency. <https://doi.org/10.1787/35fb60bd-en>.
- INL, 2013. EV project electric vehicle charging infrastructure summary Report. Idaho National Laboratory. Page 21. Web resource accessed December 2020: <https://avt.inl.gov/sites/default/files/pdf/EVProj/EVProject%20Infrastructure%20ReportJan13Dec13.pdf>.
- Jenn, Alan, Clark-Sutton, Kyle, Gallaher, Michael, Petrusa, Jeffrey, 2020. Environmental impacts of extreme fast charging. *Environ. Res. Lett.* 15 <https://doi.org/10.1088/1748-9326/ab9870>.
- Lazard, 2019. LAZARD's leveled cost OF storage analysis — version 5.0. Web resource accessed December 2020: <https://www.lazard.com/media/451087/lazards-leveled-cost-of-storage-version-50-vf.pdf>.
- Lee, Henry, Clark, Alex, 2018. Charging the future: challenges and opportunities for electric vehicle adoption. The Harvard Kennedy School, Belfer Center. Web resource accessed December 2020: https://projects.iq.harvard.edu/file/energyconsortium/files/rwp18-026_lee_1.pdf.
- Ma, C.-T., 2019. System planning of grid-connected electric vehicle charging stations and key technologies: a review. *Energies* 12 (4201). <https://doi.org/10.3390/en12214201>.
- Mai, Trieu, Jadun, Paige, Logan, Jeffrey, McMillan, Colin, Muratori, Matteo, Steinberg, Daniel, Vimmerstedt, Laura, Jones, Ryan, Haley, Benjamin, Nelson, Brent, 2018. Electrification Futures Study: Scenarios of Electric Technology Adoption and Power Consumption for the United States. National Renewable Energy Laboratory, Golden, CO. NREL/TP-6A20-71500. Web resource accessed December 2020: <https://www.nrel.gov/docs/fy18osti/71500.pdf>.
- Mallapragada, Dhari K S., Sepulveda, Nestor A., Jenkins, Jesse D., 2020. Long-run system value of battery energy storage in future grids with increasing wind and solar generation. *Appl. Energy* 275. <https://doi.org/10.1016/j.apenergy.2020.115390>.
- MIT Energy Initiative, 2019. Insights into future mobility. *MIT Energy Initiative*. Web resource, Cambridge, MA, p. 105 accessed December 2020: http://energy.mit.edu/in_sightsintofuturemobility. "Range Anxiety".
- Muratori, Matteo, 2018. Impact of uncoordinated plug-in electric vehicle charging on residential power demand. *Nat. Energy* 3. <https://doi.org/10.1038/s41560-017-0074-z>. In press.
- OPEC, 2019. "World oil outlook 2040". *Organization of the petroleum exporting countries*. Web resource accessed December 2020: https://www.opec.org/opec_web/static_files_s_project/media/downloads/publications/WOO_2018.pdf.
- Pandzić, P., Pandzić, H., Kuzle, I., 2018. Coordination of regulated and merchant energy storage investments. *IEEE Transactions on Sustainable Energy* 9 (3). <https://doi.org/10.1109/TSTE.2017.2779404>.
- Potomac Economics, 2020. 2019 state of the market Report for the ERCOT electricity markets. Web resource accessed December 2020: <http://www.potomaceconomics.com/wp-content/uploads/2020/06/2019-State-of-the-Market-Report.pdf>.
- Siirola, John Daniel, Watson, Jean-Paul, Lara, Cristiana, Grossmann, Ignacio, 2018. Grid-level modeling: opportunities and program plan. In: Conference: *Proposed For Presentation at the IDAES Stakeholder Meeting* Held May 23-24, 2018 in Washington, DC. Web resource accessed December 2020: <https://www.osti.gov/biblio/1523790>.
- Szina, Julia K., Sheppard, Colin J.R., Abhyankar, Nikit, Gopal, Anand R., 2020. Reduced grid operating costs and renewable energy curtailment with electric vehicle charge management. *Energy Pol.* 136 <https://doi.org/10.1016/j.enpol.2019.111051>.
- Tabors, R.D., He, H., Birk, M., 2016. The impact of distributed energy resources on incumbent utilities: a case study of long island, New York. In: *2016 49th Hawaii International Conference On System Sciences (HICSS)*. <https://doi.org/10.1109/HICSS.2016.321>.
- Tesla, 2020. Powerpack: utility and business energy storage. Web resource accessed December 2020: <http://www.tesla.com/powerpack>.
- Tuohy, Aidan, Yong, Taiyou, Philbrick, Russ, 2013. Multi-settlement simulation of stochastic reserve determination: project status update. In: FERC Technical Conference on Increasing Market Efficiency through Improved Software. Electric Power Research Institute. Web resource accessed December 2020: <https://www.ferc.gov/CalendarFiles/20140411131845-T4-A%20-%20Tuohy.pdf>.
- US Census, 2020. QuickFacts: Texas. Web resource accessed December 2020: <https://www.census.gov/quickfacts/TX>.
- US Federal Highway Administration, 2017. Table MV-1 - highway statistics 2017: state motor-vehicle registrations - 2017. Web resource accessed January 2021: <https://www.fhwa.dot.gov/policyinformation/statistics/2017/mv1.cfm>.
- Wolinetz, Michael, Aksen, Jonn, Peters, Jotham, Crawford, Curran, 2018. "Simulating the value of electric-vehicle-grid integration using a behaviourally realistic model". *Nature Energy* 3 (2). <https://doi.org/10.1038/s41560-017-0077-9>.
- Wu, Di, Guo, Fengdi, Field, Frank R., De Kleine, Robert, D., Kim, Hyung Chul, Wallington, Timothy J., Kirchain, Randolph E., 2019. Regional heterogeneity in the emissions benefits of electrified and lightweighted light-duty vehicles. *Environ. Sci. Technol.* 53 (18) <https://doi.org/10.1021/acs.est.9b00648>.
- Xu, Yanyan, Çolak, Serdar, Kara, Emre C., Moura, Scott J., González, Marta C., 2018. Planning for electric vehicle needs by coupling charging profiles with urban mobility. *Nature Energy* 3 (6). <https://doi.org/10.1038/s41560-018-0136-x>.
- Xu, Min, Yang, Hai, Wang, Shuaian, 2020. Mitigate the range anxiety: siting battery charging stations for electric vehicle drivers. *Transport. Res. C Emerg. Technol.* 114 <https://doi.org/10.1016/j.trc.2020.02.001>.